

Preparation of durable superhydrophobic cotton fabric for self-cleaning and oil–water separation

Qingbo Xu (✉ xuqingbo2015@yeah.net)

Anhui Polytechnic University

Xiating Ke

Fuzhou University

Zongqian Wang

Anhui Polytechnic University

Peng Wang

Anhui Polytechnic University

Changlong Li

Anhui Polytechnic University

Research Article

Keywords: Cotton fabric, Fluoropolymer, Superhydrophobic surface, Self-cleaning, Oil–water separation

Posted Date: May 10th, 2021

DOI: <https://doi.org/10.21203/rs.3.rs-364924/v1>

License:   This work is licensed under a Creative Commons Attribution 4.0 International License.

[Read Full License](#)

Version of Record: A version of this preprint was published at *Fibers and Polymers* on April 11th, 2022.
See the published version at <https://doi.org/10.1007/s12221-022-4770-3>.

Abstract

Improving the surface roughness and reducing the surface energy are the main strategies for constructing cotton fabrics with superhydrophobic surface. However, the complex finishing process and poor durability still impede the production and application of superhydrophobic cotton fabrics. Therefore, it is critical to produce superhydrophobic fabrics with excellent durability via a noncomplicated method. In this work, monomers of methyl methacrylate (MMA) and trifluoroethyl methacrylate (TFMA) were polymerized via free radical polymerization to produce a fluoropolymer. Then, the fabric was coated with the fluoropolymer to construct a superhydrophobic surface via the pad-dry-cure technology. The TFMA unit in the fluoropolymer had lower surface energy than the MMA unit. Under the high-temperature curing condition, the MMA unit in the fluoropolymer was grafted onto the cotton fabric via transesterification, and the TFMA was exposed on the fabric surface. The finished fabric showed durable superhydrophobic properties, outstanding oil–water separation properties, and excellent self-cleaning properties. Given the results, the finished fabric has great potential application in clothing and industrial fields.

Introduction

Cotton fabrics are widely used in daily life because of their excellent wearing comfort and softness (Duan et al. 2020; Xu et al. 2020d; Ye et al. 2020). With the development of science and technology, traditional cotton fabrics have been unable to meet human production and living needs; hence, a series of functional cotton fabrics, such as antibacterial cotton fabric (Gao et al. 2020; Xu et al. 2019), superhydrophobic cotton fabric (Ou et al. 2020; Yan et al. 2020), and conductive cotton fabric (Trovato et al. 2021; Zheng et al. 2020) have been explored. Among these functional fabrics, superhydrophobic fabrics have received enough attention because of their great application potential in self-cleaning and oil–water separation (Chauhan et al. 2019; Yang et al. 2020).

At present, improving surface roughness and reducing surface energy are the main strategies to construct cotton fabrics with superhydrophobic surface (Dalawai et al. 2020; Das et al. 2021; Sam et al. 2019). To improve the surface roughness of cotton fabrics, immobilizing inorganic particles such as silica (SiO_2) (Jannatun et al. 2020; Kong et al. 2020; Xu et al. 2020c), titanium dioxide (TiO_2) (Guo et al. 2020; He et al. 2020; Ren et al. 2020), and zinc oxide (ZnO) (Khan et al. 2020; Patil et al. 2019; Wang et al. 2019) on the cotton fabric surface or etching the fabric surface with chemical agents are the main preparation methods. Shang et al. (Shang et al. 2020) used hydrophobic SiO_2 nanoparticles, octavinyl polyhedral oligomeric silsesquioxane, and castor oil–based thiolated oligomer to coat cotton fabric via spray deposition and UV light–induced thiol–ene click chemistry. The SiO_2 coating could improve the surface roughness of the finished fabrics. As a result, the superhydrophobic surface of the fabrics was not destroyed even after 30 sandpaper abrasion cycles or 60 min ultrasound treatment. Ren et al. (Ren et al. 2020) used TiO_2 @SA/CS coating, comprising TiO_2 , chitosan (CS), and stearic acid (SA) to coat cotton fabric. The surface of the obtained fabric showed excellent superhydrophobicity. Moreover, the superhydrophobic surface of the modified fabrics could become superhydrophilic when the surface was

subjected to ammonia treatment, and the superhydrophobicity could be restored after heating treatment. Cheng et al. (Cheng et al. 2019b) improved the surface roughness by etching the cotton fabric with biological enzymes. Then, they coated the etched fabric surface with epoxidized soybean oil and stearic acid, thus successfully preparing superhydrophobic cotton fabric. The root-mean-square roughness of the pristine fabric was 3–8 nm, and that of the etched fabric surface was 39–45 nm, indicating that the surface roughness was successfully improved by etching the cotton fabric with biological enzymes. The root-mean-square roughness of the finished cotton fabric was 42–50 nm, indicating that the surface roughness of the cotton fabric did not reduce after the surface was coated with epoxy soybean oil and stearic acid. The finished cotton fabric showed excellent superhydrophobicity, and its water contact angle (WCA) was higher than 157.3°. Moreover, the WCA values of the finished fabric still exceeded 152.7° after it was subjected to 10 abrasion cycles or 100 tape-peeling treatment tests, demonstrating the excellent mechanical stability of the fabric. Cheng et al. (Cheng et al. 2020a) also improved the surface roughness by etching the cotton fabric with 7.5 wt% sulfuric acid solution; then, they coated the etched fabric surface with epoxidized soybean oil and stearic acid, successfully preparing superhydrophobic cotton fabric. The WCA of the obtained fabric was 155.6°. After the obtained fabric was subjected to 14 abrasion cycles or 100 tape peeling treatment times, the WCA value was still 150.0°, revealing the excellent mechanical stability of the fabric. Although the abovementioned methods improved the surface roughness of the fabric, the inorganic particles easily fell off the fabric surface, and the etching strategies greatly reduced the fabric mechanical strength. These disadvantages hinder the actual production and application of superhydrophobic cotton fabrics.

To reduce the surface energy of the cotton fabric, the main strategy involves coating the cotton fabric with some fluoropolymer (Xu et al. 2020b; Yang et al. 2018a; Yang et al. 2018b), polyester (Wang et al. 2014; Xi et al. 2016), and silane polymer (Eduok et al. 2021; Ge et al. 2020; Kim et al. 2020). Shang et al. (Shang et al. 2021) used tannic acid to treat the cotton fabric surface and then coated the treated fabric sample with aminopropylsilyl polyhedral oligomeric silsesquioxane. The modified fabric showed excellent superhydrophobic properties, and its WCA was higher than 158.3°. Moreover, the superhydrophobic properties of the modified fabrics were not significantly reduced after they were subjected to 15 abrasion cycles or 50 tape peeling cycles. Xu et al. (Xu et al. 2020a) prepared superhydrophobic fabrics by coating the cotton fabric with lauryl methacrylate and subsequent crosslinking via radio-frequency capacitance coupled plasma. The obtained fabric showed excellent superhydrophobic properties, with a WCA of 157.3°. Moreover, the superhydrophobic properties of the fabric were not significantly changed after it was subjected to 1500 abrasion cycles or 45 laundering cycles. Although the superhydrophobic cotton fabric was successfully prepared via this strategy, the methods of grafting low-surface-energy material on cotton fabrics via covalent bonding were complicated, which limits the production of superhydrophobic fabrics.

In the present work, monomers of methyl methacrylate (MMA) and trifluoroethyl methacrylate (TFMA) were polymerized via a free radical polymerization reaction to produce poly(methylene terephthalate) (PMT). Then, the PMT copolymer was grafted onto the cotton fabric via the pad-dry-cure technology. The TFMA unit in the PMT copolymer had lower surface energy than the MMA unit (Jiang et al. 2014). Under

the high-temperature curing condition, the MMA unit in the PMT copolymer was grafted onto the cotton fabric via transesterification, and the TFMA was exposed on the fabric surface. The cotton fabric grafted with the PMT copolymer via covalent bonding will result in a durable superhydrophobic surface. The superhydrophobic fabrics constructed via this strategy have great application in self-cleaning and oil-water separation.

Experimental Section

Materials

The reagents used in the experiment are described in Supporting Information (SI).

PMT synthesis

Free radical copolymerization was adopted to prepare the fluorinated copolymer. Methyl methacrylate (8.424 g, 84.13 mmol), TFMA (5.905 g, 35.13 mmol), azobisisobutyronitrile (0.276 g, 1.681 mmol), and 1,4-dioxane (36.0 mL) were stirred under nitrogen atmosphere for 30 min, and then the copolymerization reaction was performed at 90°C for 6 h. The purified copolymer was filtered, washed with 1,4-dioxane (50 mL × 3 times), and vacuum-dried at 100°C for 4 h to obtain the PMT.

Fabrication of superhydrophobic fabrics

First, the PMT copolymer (1 g) was dissolved in acetone (100 mL), and the solution was stirred for 30 min. Second, cotton fabric (5 cm × 5 cm) was immersed in the solution for 5 min, and the wet pick-up of fabric was controlled to 100%. Afterward, the sample was heated at 180°C for 5 min. Finally, the treated fabric sample was washed with acetone (50 mL × 3 times) and dried at 100°C for 1 h. The finished fabric sample was named SC-1. Samples SC-2 and SC-3 had 2 wt% and 3 wt% PMT solution concentrations, respectively, but their preparation processes were similar to that of SC-1.

Characterization

The methods for the structure and property characterization of the fabrics are described in Supporting Information.

Results And Discussion

Structural analysis of PMT copolymer

The synthesis route of PMT copolymer is shown in Fig. 1. The azobisisobutyronitrile initiates the copolymerization of MMA monomer and TFMA monomer under the condition of oxygen isolation to form the PMT copolymer. To analyze the PMT copolymer structure, Fourier-transform infrared (FTIR) spectroscopy and proton nuclear magnetic resonance spectroscopy analysis were performed. Fig. S1 shows the FTIR spectra of the PMT copolymer. The peaks at 1741 cm^{-1} and 1171 cm^{-1} were due to the

stretching vibrations of C = O and C-F₃ bonds, respectively. Moreover, the peak of the C = C bond vibration was not present in the spectra, indicating that the copolymerization of the MMA and TFMA was finished. The ¹H NMR spectra of the PMT copolymer are displayed in Fig. S2. The chemical shifts at 3.63 ppm (a, -CH₂-CF₃) and 4.63 ppm (b, -CH₃) are assigned to the TFMA and MMA units, respectively. These results demonstrate that the PMT copolymer was successfully synthesized using the MMA and TFMA monomers.

Surface structure and morphology analysis of the finished fabrics

The preparation route and the mechanism of the finished fabrics are displayed in Fig. 2. In the preparation process, the pad-dry-cure technology was used to prepare the finished fabrics. First, the cotton fabric was immersed in the PMT solution and then heated at 180°C for 5 min; the obtained fabric was finally washed with acetone to remove the unreacted PMT copolymer, thus finishing the fabric with PMT copolymer. Moreover, the TFMA chain in the PMT copolymer had lower surface energy than the MMA chain. Under the high-temperature heating condition, the MMA chain reacted with the hydroxyl groups of the cotton fiber via transesterification, while the TFMA chain tended to be more exposed on the fabric surface (Jiang et al. 2014). Consequently, the MMA chain of the PMT copolymer was grafted onto the fabric sample via covalent bonding, and the TFMA chain on the cotton fabric could construct the superhydrophobic surface. To verify the reaction mechanism between PMT copolymer and cotton fabric, the structure and morphology of the finished fabric were analyzed.

The attenuated total reflection (ATR) spectra of pristine and finished fabric samples are displayed in Fig. 3. Compared with the spectrum of the pristine fabric, those of three finished fabrics had new peaks at 1742 cm⁻¹ and 1102 cm⁻¹, assigned to the stretching vibrations of the C = O group and C-F₃ group, respectively. This result demonstrates that the finished fabrics were successfully coated with the PMT copolymer.

To further analyze the surface structure of fabric samples, X-ray photoelectron spectroscopy (XPS) analysis was conducted. Figure 4a shows the wide-range XPS spectra of the pristine and finished fabrics. The spectrum of the pristine fabric had peaks at 283.6 eV and 531.8 eV, assigned to the C 1s and O 1s signals, respectively (Zhou et al. 2019). Compared with the spectrum of the pristine fabric, those of the three finished fabrics had an additional peak at 687.4 eV, attributed to the F 1s signal (Chen et al. 2019). This result also indicates that the finished fabrics were coated with the PMT copolymer.

Figure 4b shows the F 1s XPS spectra of the fabrics. Sample SC-3 featured the highest peak intensity of F signal on the finished fabric surface, while SC-1 had the lowest. Moreover, the F content on the finished fabric surface also showed a similar trend (Table S1). This result demonstrates that the content of PMT copolymer coated on the finished fabric surface increased with the concentration of PMT copolymer solution during the experiment. Figures 4c–f show the C 1s XPS spectra of the pristine and finished fabrics. The spectrum of the pristine fabric had peaks at 284.5 eV (C-C), 286.3 eV (C-OH), and 288.4 eV (C-O-C) (Ding et al. 2019; Shang et al. 2021), while the spectra of the three finished fabrics had a new

peak at 292.0 eV (C-F₃) (Yang et al. 2018b). Moreover, the peak at 288.6 eV (C = O/C-O-C) of the three finished fabrics was slightly shifted compared with that of the pristine fabric. This result indicates that the finished fabric surface produced a new C = O valence bond. According to the ATR and XPS results, the PMT copolymer was successfully grafted onto the finished fabrics via transesterification.

Figure 5 shows the XRD spectra of the pristine and finished fabrics. The three finished fabrics showed cellulose peaks at 15.1°, 16.6°, 23.0°, and 34.6°, similar to the pristine fabric (Luo et al. 2021; Tian et al. 2019). This result demonstrates that the cotton fiber crystal structure was not significantly destroyed after the finishing process.

Figure 6 shows the scanning electron microscopy (SEM) image of the pristine and finished fabrics. In the low-magnification SEM images (Figs. 6a–d), the three finished fabrics were similar to the pristine fabric. This result indicates that the PMT copolymer was mainly grafted onto the cotton fibers, and it did not cover the gap between the fibers, which ensured that the finished fabric had excellent air permeability. In the high-magnification SEM images (Figs. 6e–l), the surface of the pristine fabric appeared clean and smooth, while the surfaces of the three finished fabrics were rough and had many filaments. Moreover, among the three finished fabric samples, SC-2 had the roughest surface. To prove that the filaments on the surface of the finished fabrics were the PMT copolymer, the elements on the SC-2 surface and their distribution were analyzed. As shown in Figs. 6m–p, the SC-2 surface contained C, O, and F, indicating that the filaments on SC-2 were the PMT copolymer. In addition, the C, O, and F element mapping images also demonstrate that the PMT copolymer was uniformly dispersed on the SC-2 surface. The above results prove that the PMT copolymer was successfully coated and uniformly distributed on the finished fabrics.

Analysis of superhydrophobic properties of fabric samples

The above structural analysis of the finished fabric shows that the PMT was successfully grafted onto the fabric. To analyze the superhydrophobic properties of the finished fabric, which was coated with the PMT copolymer, the pristine and finished fabrics were compared. As shown in Figs. 7a–d, the water droplet (stained with methyl orange, MO) was quickly wetted on the surface of the pristine fabric, while it exhibited a spherical shape on the surfaces of the three finished fabrics. To quantify the hydrophobic properties of the fabrics, the WCAs were determined (Figs. 7e–h). Distilled water was quickly wetted on the pristine fabric; therefore, the WCA of the pristine fabric was 0°. The WCAs of the three finished fabrics were higher than 155.0°, while that of the pristine fabric was lower. Moreover, among the three finished fabrics, SC-2 had the highest WCA (161.0° ± 0.2°). Therefore, SC-2 was selected as the research object to analyze the hydrophobic performance and oil–water separation performance of the fabric. Another interesting comparison between the pristine and finished fabrics is illustrated in Figs. 7i and j. Droplets of common liquids in daily life, such as milk and coffee, appeared spherical on the SC-2 surface, but rapidly melted on the surface of the pristine fabric.

Figures 8a and b show optical images of the pristine fabric and SC-2 placed on water (stained with ink). The pristine fabric was immediately immersed up to the water bottom, while the SC-2 remained afloat on the water surface even after long periods. Figures 8c and d show optical images of the pristine fabric and SC-2 after water immersion. The SC-2 had a bright, shining surface (Fig. 8c), while the surface of pristine fabric was not different from that before the immersion (Fig. 8d). The photograph of the stream water bouncing off the SC-2 surface is displayed in Fig. 8e. The flowing water immediately bounced off the SC-2 surface without any wetting trace on the surface. According to these results, a superhydrophobic surface was successfully constructed by grafting PMT copolymer onto fabrics.

Self-cleaning properties of finished fabrics

The finished fabric had excellent superhydrophobic properties, meaning that it had great application potential in self-cleaning. Figures 9a and b show optical images of the pristine fabric and SC-2 immersed in polluted water. The pristine fabric became contaminated immediately after its immersion (Fig. 9a). However, the surface of the SC-2 remained clean even after its immersion (Fig. 9b). The self-cleaning properties of the pristine fabric and SC-2 are also compared in Fig. 9c. Methyl orange dust was placed on the surfaces of the pristine fabric and SC-2, and then the fabric surfaces were rinsed with distilled water. The MO dust on the SC-2 surface was easily washed away by distilled water, and no water trace was left on the fabric surface; however, a large amount of water was needed to wash off the MO dust on the surface of the pristine fabric. The results demonstrate that SC-2 had excellent self-cleaning properties for both contaminated solutions and dust pollutants.

Durability properties of the superhydrophobic surface of finished fabrics

In practical applications, the durability of the superhydrophobic fabric is a major factor. Figures 9e and f demonstrate the mechanical durability of SC-2. As shown in Fig. 9e, the WCA of the SC-2 surface decreased only slightly with the increase in the number of abrasion cycles. Even after 1600 abrasion cycles, the WCA was still $157^\circ \pm 0.5^\circ$. This indicates that the abrasion treatment had little effect on the SC-2 superhydrophobic surface. Figure 9f shows the laundering durability of the SC-2 sample. The effect of washing treatment on the durability of the SC-2 superhydrophobic surface was similar to the effect of abrasion treatment. The WCA of the SC-2 surface decreased with increasing washing runs. After 50 washing cycles, the WCA value was still $155.6^\circ \pm 0.3^\circ$. This result proves that the washing treatment had little effect on the SC-2 superhydrophobic surface. According to these results, the superhydrophobic surface of the finished fabric had excellent mechanical durability.

Analysis of oil–water separation properties of finished fabrics

The excellent durability of the finished fabric indicates that it has great application potential in the field of oil–water separation. To judge whether the finished fabric had oil–water separation properties, qualitative characterization was conducted, and the results are shown in Figs. 10a–c. The water droplets (stained with ink) and the oil droplets (stained with oil red O) were quickly wetted on the pristine fabric, while the water droplets exhibited a spherical shape on the SC-2 surface whether it wetted by the oil droplets. This

result demonstrates that the SC-2 can be used for oil–water separation processes. Figure 10d shows the separation efficiencies of various oil–water mixtures when SC-2 was used as the filter material. The separation efficiency of the various oil–water mixtures such as cyclohexane/water mixtures and N-hexane/water mixtures was 99.5%. Moreover, the WCA of SC-2 after it was subjected to various oil–water separation processes also exceeded 156.0° (Fig. 10e). These results indicate that the finished fabric had excellent oil–water separation properties.

Analysis of desired properties of fabrics

In practical applications, the inherent properties of modified fabric samples are critical (Xu et al. 2017; Xu et al. 2018; Zhang et al. 2018). Hence, the water vapor permeability, water absorption ability, tensile strength, elongation, and flexibility of the fabric samples were analyzed, and the results are depicted in Fig. 11.

The water vapor permeabilities of the three finished fabrics were slightly lower than that of the pristine fabric, by 11.0% at most (Fig. 11(1)). The water absorption abilities of the three finished fabrics were similar to that of the pristine fabric (Fig. 11(2)). The tensile breaking strengths of the three finished fabrics were lower than that of the pristine fabric (Fig. 11(3)), but by 16.6% at most. The elongations of the three finished fabrics were almost the same as that of the pristine fabric (Fig. 11(4)). The flexibilities of the pristine and finished fabrics are shown in Fig. 11(5). The pristine fabric showed good flexibility, and the loop height was 9.0 mm, while the loop heights of the three finished fabrics were only slightly higher. This result shows that the flexibilities of the three finished fabrics were slightly lower than that of the pristine fabric, but by an acceptable percentage. In general, the desired properties of the finished fabric were not significantly reduced after the modification.

Conclusion

A durable superhydrophobic surface of finished antibacterial fabric was successfully constructed using PMT copolymer. The finished fabric samples showed excellent superhydrophobic properties. The WCA value of the fabric with 2 wt% PMT solution (SC-2) was $161.0^\circ \pm 0.2^\circ$. The superhydrophobic surface of SC-2 also showed excellent mechanical durability. Even after SC-2 was subjected to 1600 abrasion cycles or 50 laundering cycles, the WCA values were still greater than 155.6° . Moreover, the finished fabric had excellent self-cleaning properties for both liquid and solid dust pollutants. The SC-2 sample as a filter material also showed excellent oil–water separation properties for various oil–water mixtures such as chloroform/water and N-hexane/water mixtures, and the separation efficiency was up to 99.5%. In addition, the desired properties of finished fabrics such as flexibility, air permeability, and water absorption ability were not significantly lower than those of the pristine fabric. Given the results, the finished fabric grafted with PMT copolymer has great application prospects in several fields, including self-cleaning and oil–water separation.

Declarations

Acknowledgments

This work was financially supported by the National Natural Science Foundation of China (Nos. 51873195 and 51573167).

Compliance with ethical standards

Conflict of interest: The authors declare that they have no conflict of interest.

References

- Chauhan P, Kumar A, Bhushan B (2019) Self-cleaning, stain-resistant and anti-bacterial superhydrophobic cotton fabric prepared by simple immersion technique. *J. Colloid Interf. Sci.* 535:66-74.
- Cheng QY, Zhao XL, Li YD, Weng YX, Zeng JB (2019a) Robust and nanoparticle-free superhydrophobic cotton fabric fabricated from all biological resources for oil/water separation. *Int. J. Biol. Macromol.* 140:1175-1182.
- Cheng QY, Zhao X L, Weng YX, Li YD, Zeng JB (2019b) Fully sustainable, nanoparticle-free, fluorine-free, and robust superhydrophobic cotton fabric fabricated via an eco-friendly method for efficient oil/water separation. *ACS Sustain. Chem. Eng.* 7:15696-15705.
- Chen T, Hong J, Peng C, Chen G, Yuan C, Xu Y, Dai L (2019) Superhydrophobic and flame retardant cotton modified with DOPO and fluorine-silicon-containing crosslinked polymer. *Carbohydr. Polym.* 208:14-21.
- Dalawai SP, Aly MAS, Latthe SS, Xing R, Sutar RS, Nagappan S, Liu S (2020) Recent advances in durability of superhydrophobic self-cleaning technology: A critical review. *Prog. Org. Coat.* 138:105381.
- Das A, Shome A, Manna U (2021) Porous and reactive polymeric interfaces: an emerging avenue for achieving durable and functional bio-inspired wettability. *J. Mater. Chem. A* 9:824-856.
- Ding X, Wang Y, Xu R, Qi Q, Wang W, Yu D (2019) Layered cotton/rGO/NiWP fabric prepared by electroless plating for excellent electromagnetic shielding performance. *Cellulose* 26:8209-8223.
- Duan P, Xu Q, Zhang X, Chen J, Zheng W, Li L, Liu X (2020) Naturally occurring betaine grafted on cotton fabric for achieving antibacterial and anti-protein adsorption functions. *Cellulose* 27:6603-6615.
- Eduok U, Faye O, Szpunar J, Khaled M (2021) Effect of silylating agents on the superhydrophobic and self-cleaning properties of siloxane/polydimethylsiloxane nanocomposite coatings on cellulosic fabric filters for oil–water separation. *RSC Adv.* 11:9586-9599.
- Gao D, Li Y, Lyu B, Jin D, Ma J (2020) Silicone quaternary ammonium salt based nanocomposite: a long-acting antibacterial cotton fabric finishing agent with good softness and air permeability. *Cellulose* 27:1055-1069.

- Ge M, Cao C, Liang F, Liu R, Zhang Y, Zhang W, Lai Y (2020) A "PDMS-in-water" emulsion enables mechanochemically robust superhydrophobic surfaces with self-healing nature. *Nanoscale Horiz.* 5:65-73.
- Guo W, Wang X, Huang J, Zhou Y, Cai W, Wang J, Hu Y (2020) Construction of durable flame-retardant and robust superhydrophobic coatings on cotton fabrics for water-oil separation application. *Chem. Eng. J.* 398:125661.
- He T, Zhao H, Liu Y, Zhao C, Wang L, Wang H, Wang H (2020) Facile fabrication of superhydrophobic Titanium dioxide-composited cotton fabrics to realize oil-water separation with efficiently photocatalytic degradation for water-soluble pollutants. *Colloid. Surface. A* 585:124080.
- Jannatun N, Taraqqi-A-Kamal A, Rehman R, Kuker J, Lahiri SK (2020) A facile cross-linking approach to fabricate durable and self-healing superhydrophobic coatings of SiO₂-PVA@ PDMS on cotton textile. *Eur. Polym. J.* 134:109836.
- Jiang B, Zhang L, Liao B, Pang H (2014) Self-assembly of well-defined thermo-responsive fluoropolymer and its application in tunable wettability surface. *Polymer* 55:5350-5357.
- Khan MZ, Militky J, Baheti V, Fijalkowski M, Wiener J, Voleský L, Adach K (2020) Growth of ZnO nanorods on cotton fabrics via microwave hydrothermal method: effect of size and shape of nanorods on superhydrophobic and UV-blocking properties. *Cellulose* 27:10519-10539.
- Kim S, Lee JW, Hwang W (2020) One-step eco-friendly superhydrophobic coating method using polydimethylsiloxane and ammonium bicarbonate. *ACS Appl Mater Interfaces* 12:28869-28875.
- Kong X, Zhu C, Lv J, Zhang J, Feng J (2020) Robust fluorine-free superhydrophobic coating on polyester fabrics by spraying commercial adhesive and hydrophobic fumed SiO₂ nanoparticles. *Prog. Org. Coat.* 138:105342.
- Luo Y, Wang S, Du X, Du Z, Cheng X, Wang H (2021) Durable flame retardant and water repellent cotton fabric based on synergistic effect of ferrocene and DOPO. *Cellulose* 1-18.
- Ou J, Wang F, Li W, Yan M, Amirfazli A (2020) Methyltrimethoxysilane as a multipurpose chemical for durable superhydrophobic cotton fabric. *Prog. Org. Coat.* 146:105700.
- Patil GD, Patil AH, Jadhav SA, Patil CR, Patil PS (2019) A new method to prepare superhydrophobic cotton fabrics by post-coating surface modification of ZnO nanoparticles. *Mater. Lett.* 255:126562.
- Ren J, Tao F, Liu L, Wang X, Cui Y (2020) A novel TiO₂@ stearic acid/chitosan coating with reversible wettability for controllable oil/water and emulsions separation. *Carbohydr. Polym.* 232:115807.
- Sam EK, Sam DK, Lv X, Liu B, Xiao X, Gong S, Liu J (2019) Recent development in the fabrication of self-healing superhydrophobic surfaces. *Chem. Eng. J.* 373:531-546.

- Shang Q, Hu L, Yang X, Hu Y, Bo C, Pan Z, Zhou Y (2021) Superhydrophobic cotton fabric coated with tannic acid/polyhedral oligomeric silsesquioxane for highly effective oil/water separation. *Prog. Org. Coat.* 154:106191.
- Shang Q, Liu C, Chen J, Yang X, Hu Y, Hu L, Ren X (2020) Sustainable and robust superhydrophobic cotton fabrics coated with castor oil-based nanocomposites for effective oil–water separation. *ACS Sustain. Chem. Eng.* 8:7423-7435.
- Tian P, Liu M, Wan C, Zhang G, Zhang F (2019) Synthesis of a formaldehyde-free flame retardant for cotton fabric. *Cellulose* 26:9889-9899.
- Trovato V, Teblum E, Kostikov Y, Pedrana A, Re V, Nessim GD, Rosace G (2021) Electrically conductive cotton fabric coatings developed by silica sol-gel precursors doped with surfactant-aided dispersion of vertically aligned carbon nanotubes fillers in organic solvent-free aqueous solution. *J. Colloid Interf. Sci.* 586:120-134.
- Wang L, Xi GH, Wan SJ, Zhao CH, Liu XD (2014) Asymmetrically superhydrophobic cotton fabrics fabricated by mist polymerization of lauryl methacrylate. *Cellulose* 21:2983-2994.
- Wang M, Peng M, Weng YX, Li YD, Zeng JB (2019) Toward durable and robust superhydrophobic cotton fabric through hydrothermal growth of ZnO for oil/water separation. *Cellulose* 26:8121-8133.
- Xi G, Wang J, Luo G, Zhu Y, Fan W, Huang M, Liu X (2016) Healable superhydrophobicity of novel cotton fabrics modified via one-pot mist copolymerization. *Cellulose* 23:915-927.
- Xu L, Guo Y, Liu L, Bai G, Shi J, Zhang L, Yu J (2020a) Fabrication of fluorine-free, comfortable and wearable superhydrophobic fabrics via capacitance coupled plasma with methyl side-chain lauryl methacrylate coatings. *Prog. Org. Coat.* 146:105727.
- Xu Q, Ke X, Cai D, Zhang Y, Fu F, Endo T, Liu X (2018) Silver-based, single-sided antibacterial cotton fabrics with improved durability via an l-cysteine binding effect. *Cellulose* 25:2129-2141.
- Xu Q, Shen L, Duan P, Zhang L, Fu F, Liu X (2020b) Superhydrophobic cotton fabric with excellent healability fabricated by the “grafting to” method using a diblock copolymer mist. *Chem. Eng. J.* 379:122401.
- Xu Q, Wang L, Fu F, Liu X (2020c) Fabrication of fluorine-free superhydrophobic cotton fabric using fumed silica and diblock copolymer via mist modification. *Prog. Org. Coat.* 148:105884.
- Xu Q, Xie L, Diao H, Li F, Zhang Y, Fu F, Liu X (2017) Antibacterial cotton fabric with enhanced durability prepared using silver nanoparticles and carboxymethyl chitosan. *Carbohydr. Polym.* 177:187-193.
- Xu Q, Yang J, Zhang X, Wen X, Yamada M, Fu F, Liu X (2020d) A “grafting through” strategy for constructing Janus cotton fabric by mist polymerization. *J. Mater. Chem. A* 8:24553-24562.

- Xu Q, Zheng W, Duan P, Chen J, Zhang Y, Fu F, Liu X (2019). One-pot fabrication of durable antibacterial cotton fabric coated with silver nanoparticles via carboxymethyl chitosan as a binder and stabilizer. *Carbohydr. Polym.* 204:42-49.
- Yang M, Liu W, Liang L, Jiang C, Liu C, Xie Y, Pi K (2020) A mild strategy to construct superhydrophobic cotton with dual self-cleaning and oil–water separation abilities based on TiO₂ and POSS via thiol-ene click reaction. *Cellulose* 27:2847-2857.
- Yang M, Liu W, Jiang C, He S, Xie Y, Wang Z (2018a) Fabrication of superhydrophobic cotton fabric with fluorinated TiO₂ sol by a green and one-step sol-gel process. *Carbohydr. Polym.* 197:75-82.
- Yang M, Liu W, Jiang C, Liu C, He S, Xie Y, Wang Z (2018b) Facile preparation of robust superhydrophobic cotton textile for self-cleaning and oil–water separation. *Ind. Eng. Chem. Res.* 58:187-194.
- Yan X, Zhu X, Ruan Y, Xing T, Chen G, Zhou C (2020) Biomimetic, dopamine-modified superhydrophobic cotton fabric for oil–water separation. *Cellulose* 27:7873-7885.
- Ye Z, Li S, Zhao S, Deng L, Zhang J, Dong A (2020). Textile coatings configured by double-nanoparticles to optimally couple superhydrophobic and antibacterial properties. *Chem. Eng. J.* 127680.
- Zhang S, Yang X, Tang B, Yuan L, Wang K, Liu X, Chen S (2018) New insights into synergistic antimicrobial and antifouling cotton fabrics via dually finished with quaternary ammonium salt and zwitterionic sulfobetaine. *Chem. Eng. J.* 336:123-132.
- Zheng Y, Yin R, Zhao Y, Liu H, Zhang D, Shi X, Shen C (2020) Conductive MXene/cotton fabric based pressure sensor with both high sensitivity and wide sensing range for human motion detection and E-skin. *Chem. Eng. J.* 127720.
- Zhou Q, Yan B, Xing T, Chen G (2019) Fabrication of superhydrophobic caffeic acid/Fe@ cotton fabric and its oil-water separation performance. *Carbohydr. Polym.* 203:1-9.

Figures

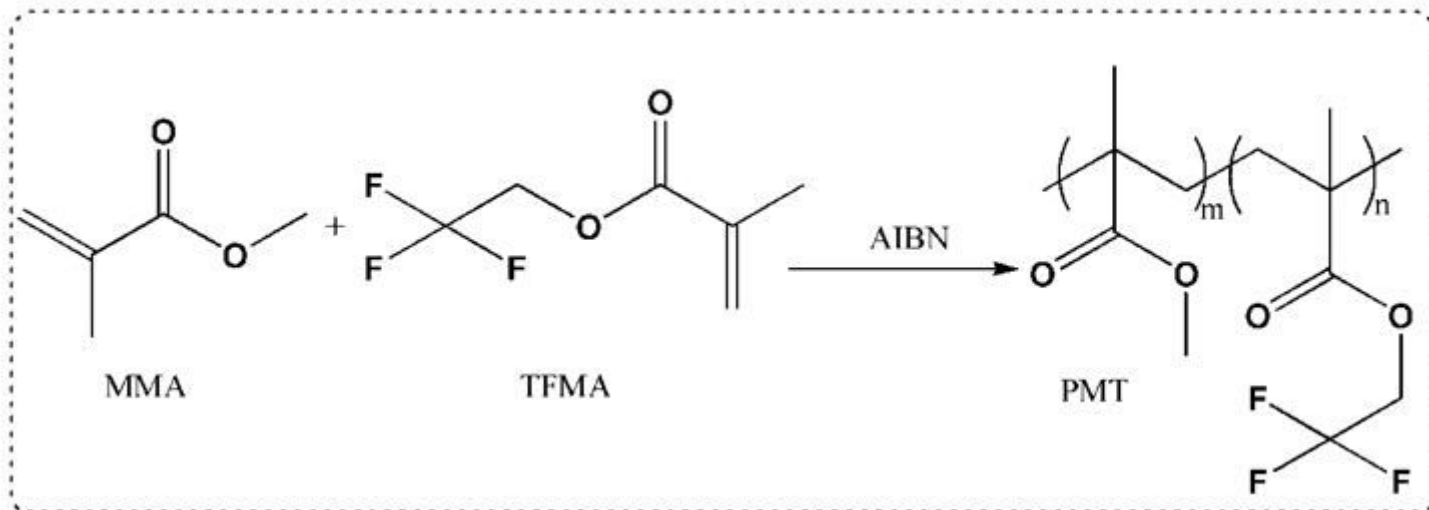


Figure 1

PMT synthesis route.

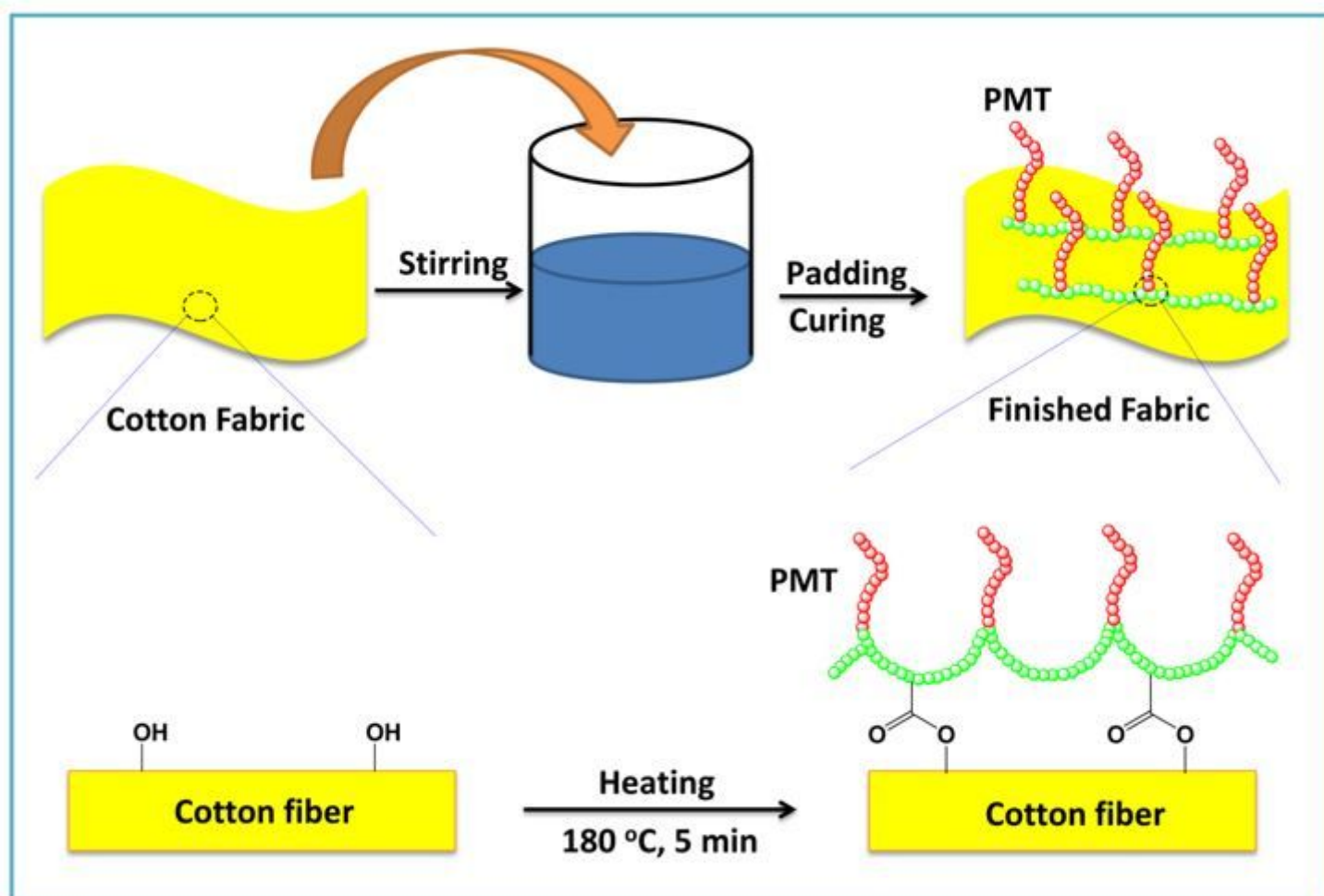


Figure 2

Preparation route and mechanism of the finished fabric.

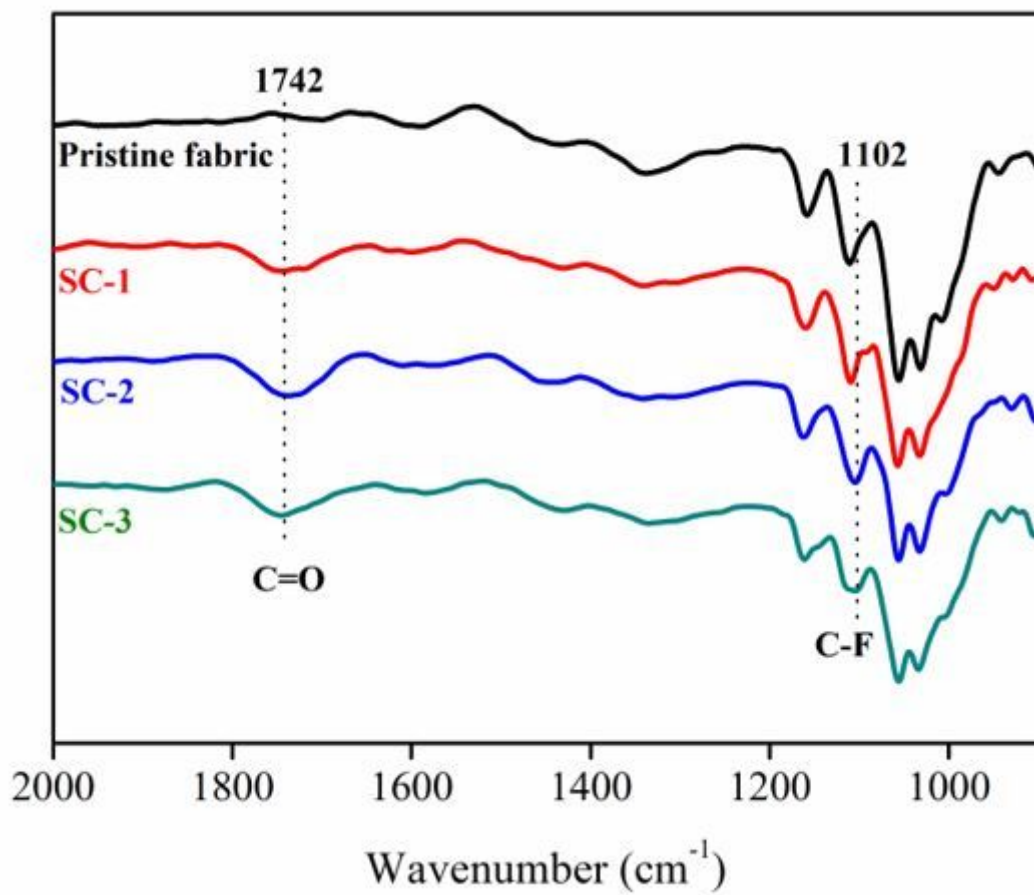


Figure 3

ATR-FTIR spectra of fabrics.

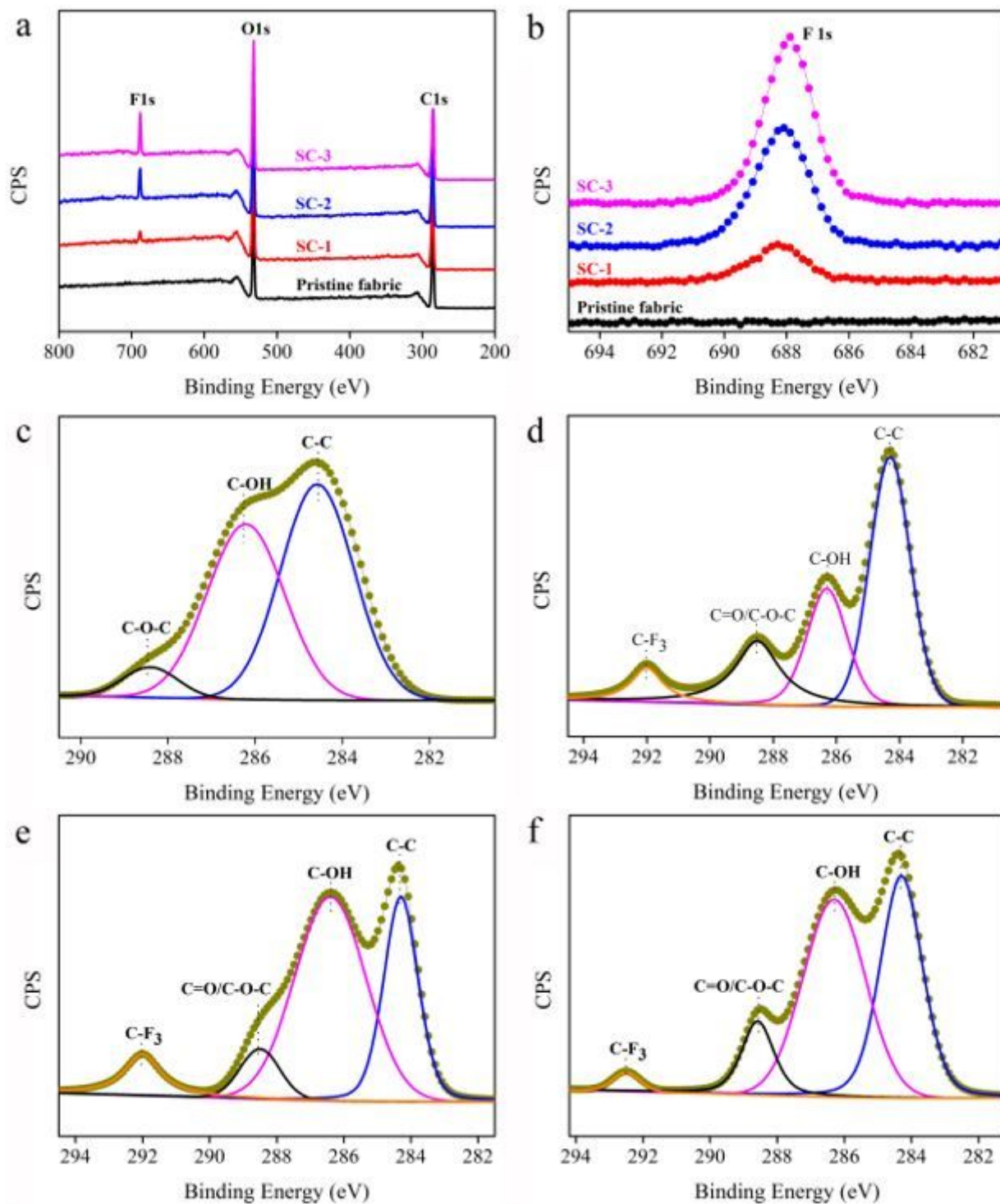


Figure 4

Wide-range XPS spectra and C 1s XPS spectra of the pristine fabric (a, e); SC-1 (b, f); SC-2 (c, g); and SC-3 (d, h). F 1s XPS spectra of the fabric samples (i).

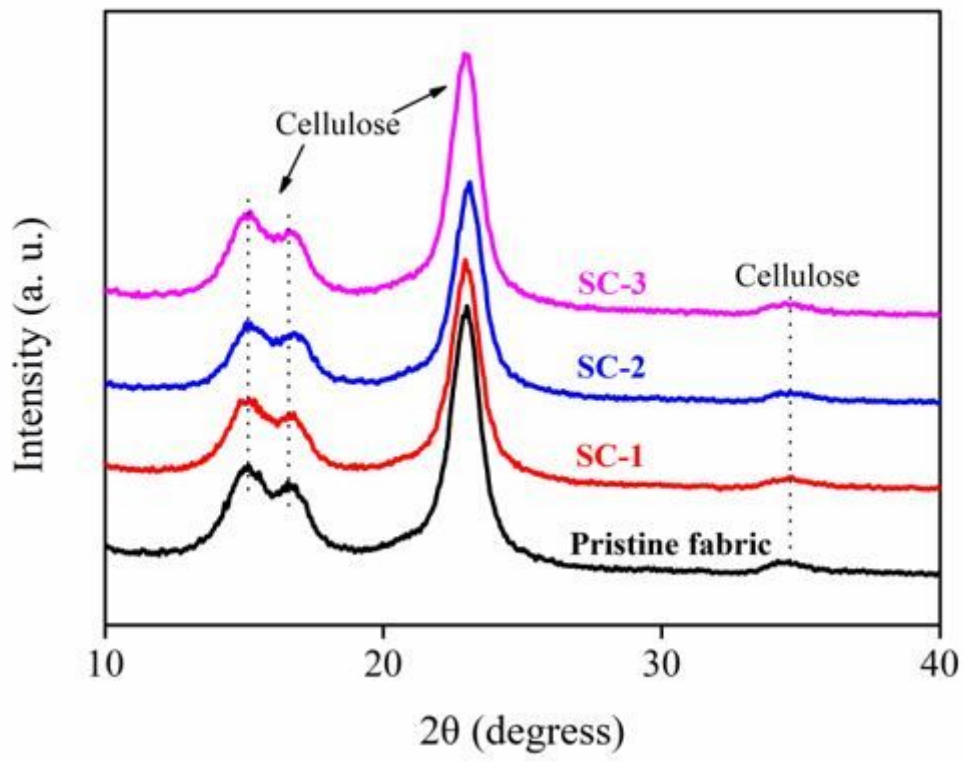


Figure 5

XRD spectra of fabric samples.

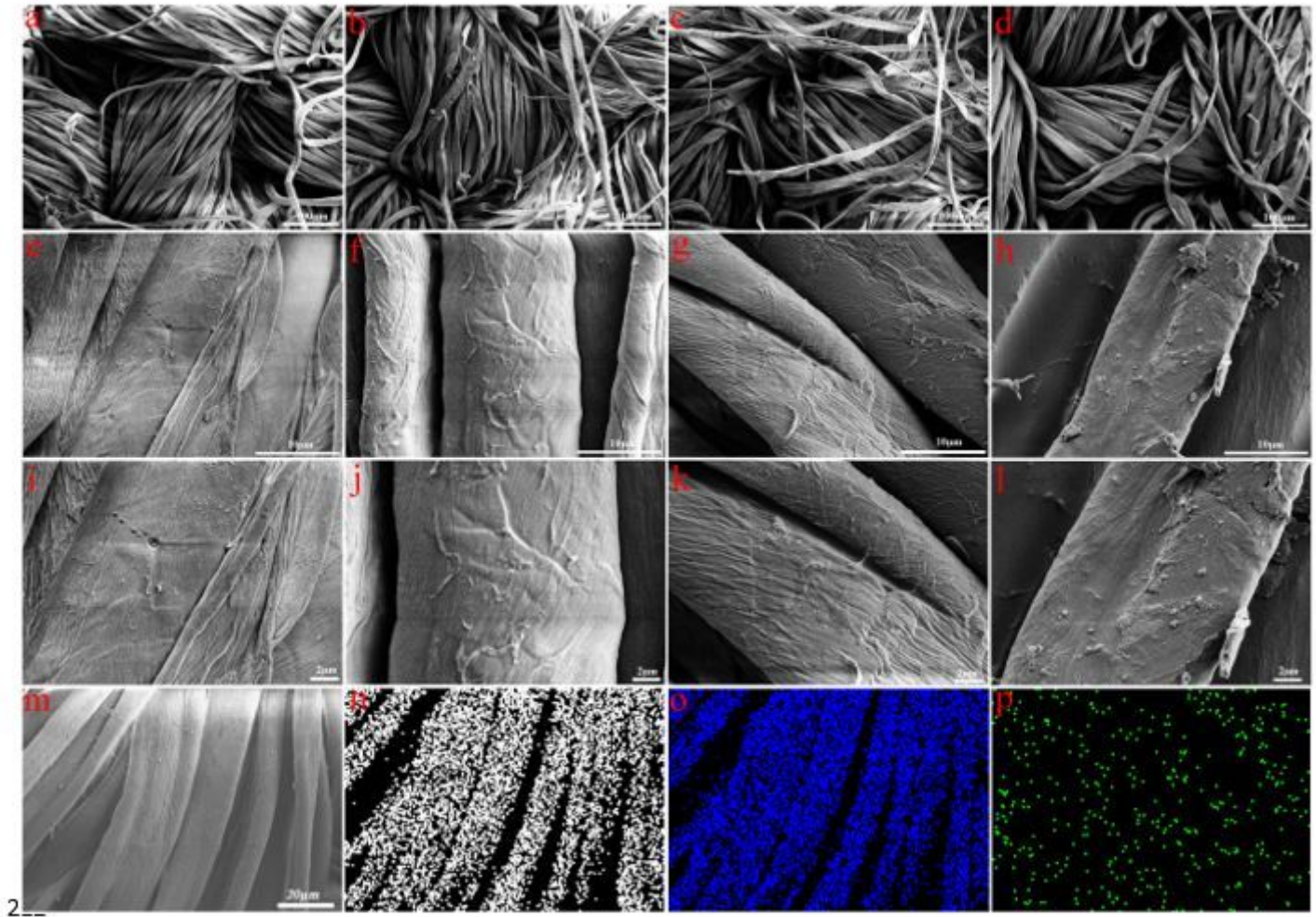


Figure 6

SEM images of the pristine fabric (a, e, i); SC-1 (b, f, j); SC-2 (c, g, k); and SC-3 (d, h, l). SEM image (m), C (n), O (o), and F (p) element mapping images.

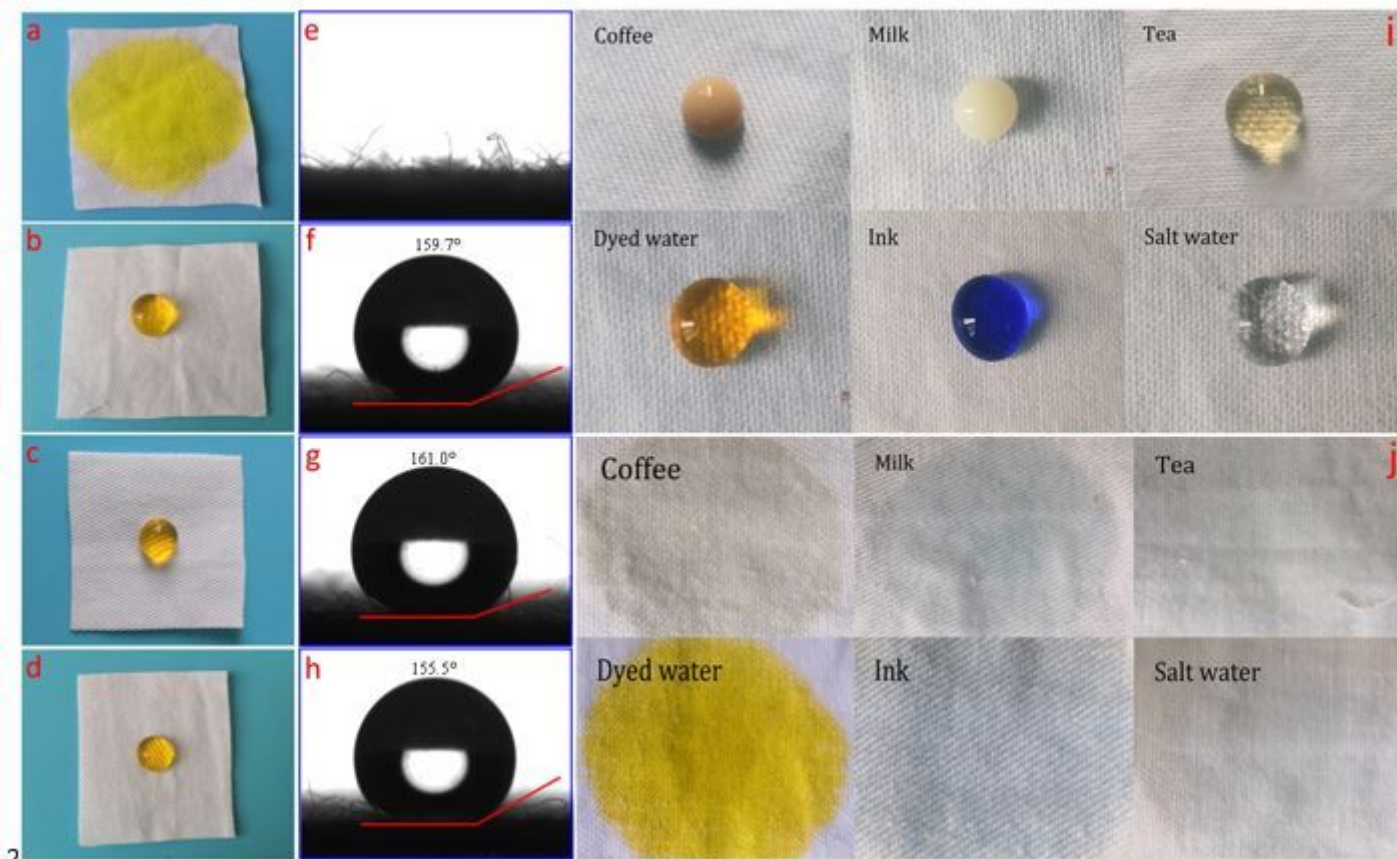


Figure 7

Water droplet (stained with methyl orange) placed on fabrics and water contact angle image of fabric samples: pristine fabric (a, e); SC-1 (b, f); SC-2 (c, g); and SC-3 (d, h). Optical image of droplets of several common liquids placed on SC-2 (i) and pristine fabric (j).

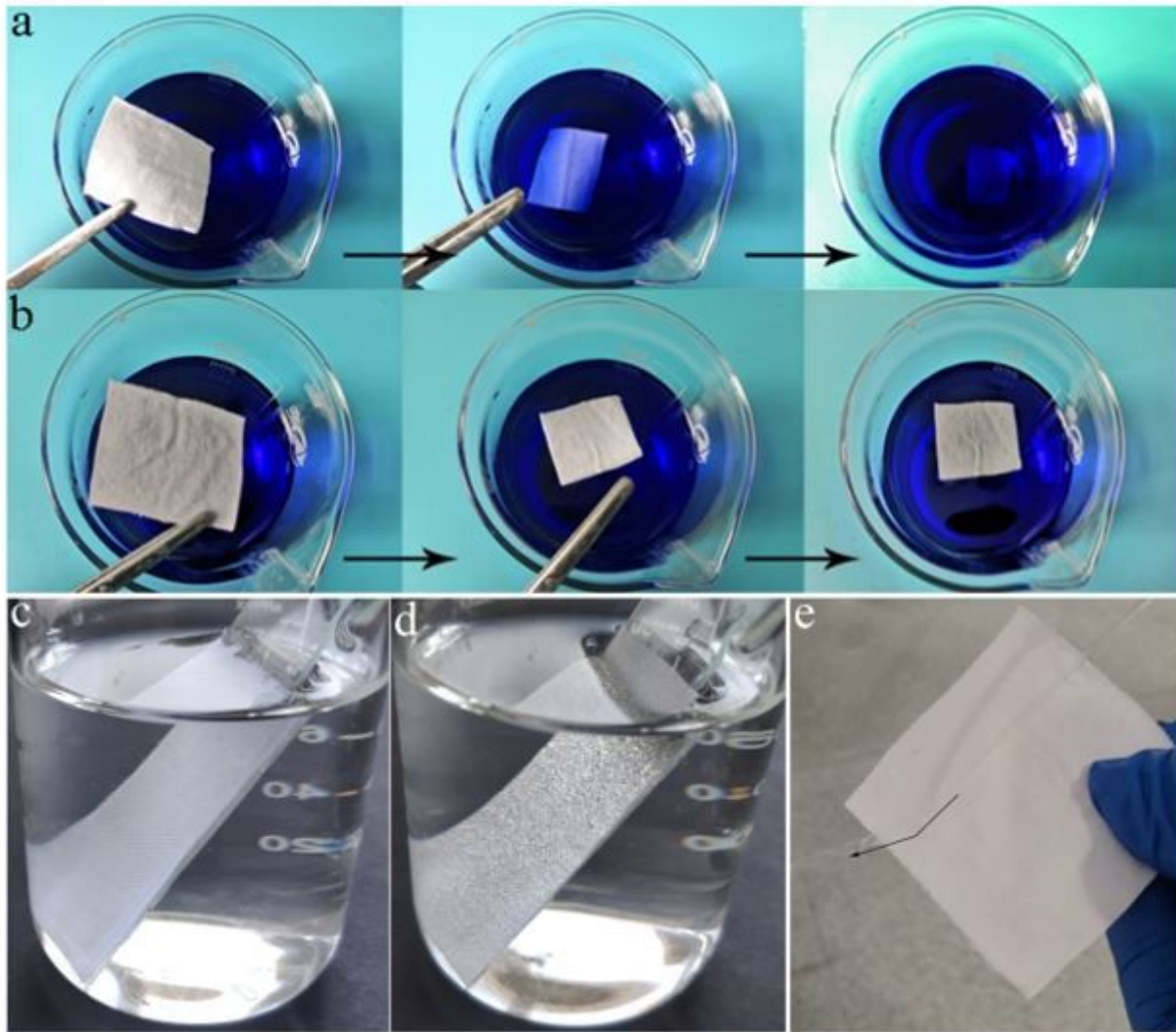


Figure 8

The pristine fabric immersed in water (a) and SC-2 afloat on water (b). The shining surface of SC-2 in water (c) and the surface of the pristine fabric wetted by water (d). Flowing water bouncing off the SC-2 surface (e).

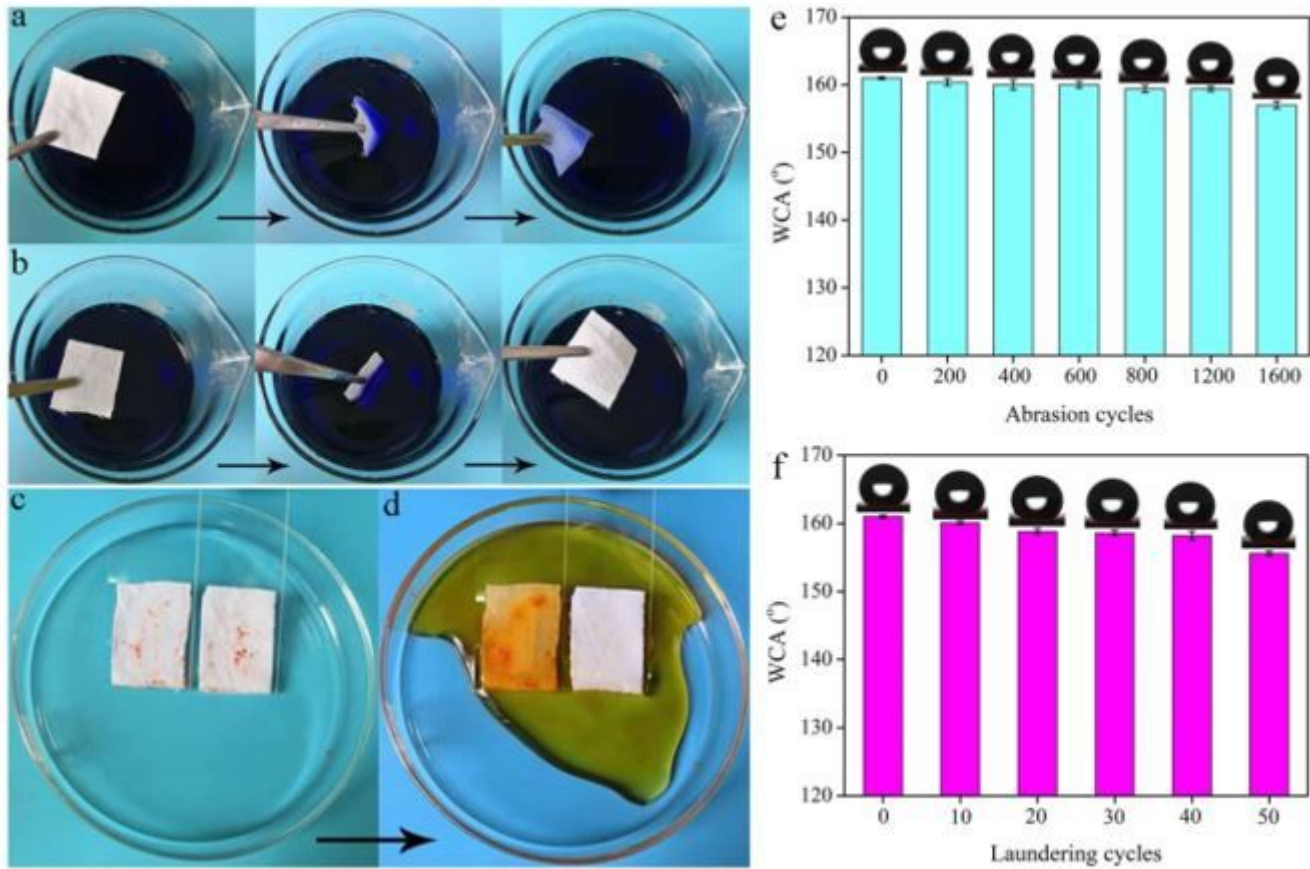


Figure 9

Self-cleaning of the pristine fabric (a) and SC-2 (b) treated with stained water. Self-cleaning behavior of solid dust on the surface of the pristine fabric (c) and SC-2 (d). Durability of SC-2 subjected to abrasion cycles (e) and laundering cycles (f). Analysis of oil–water separation properties of finished fabrics

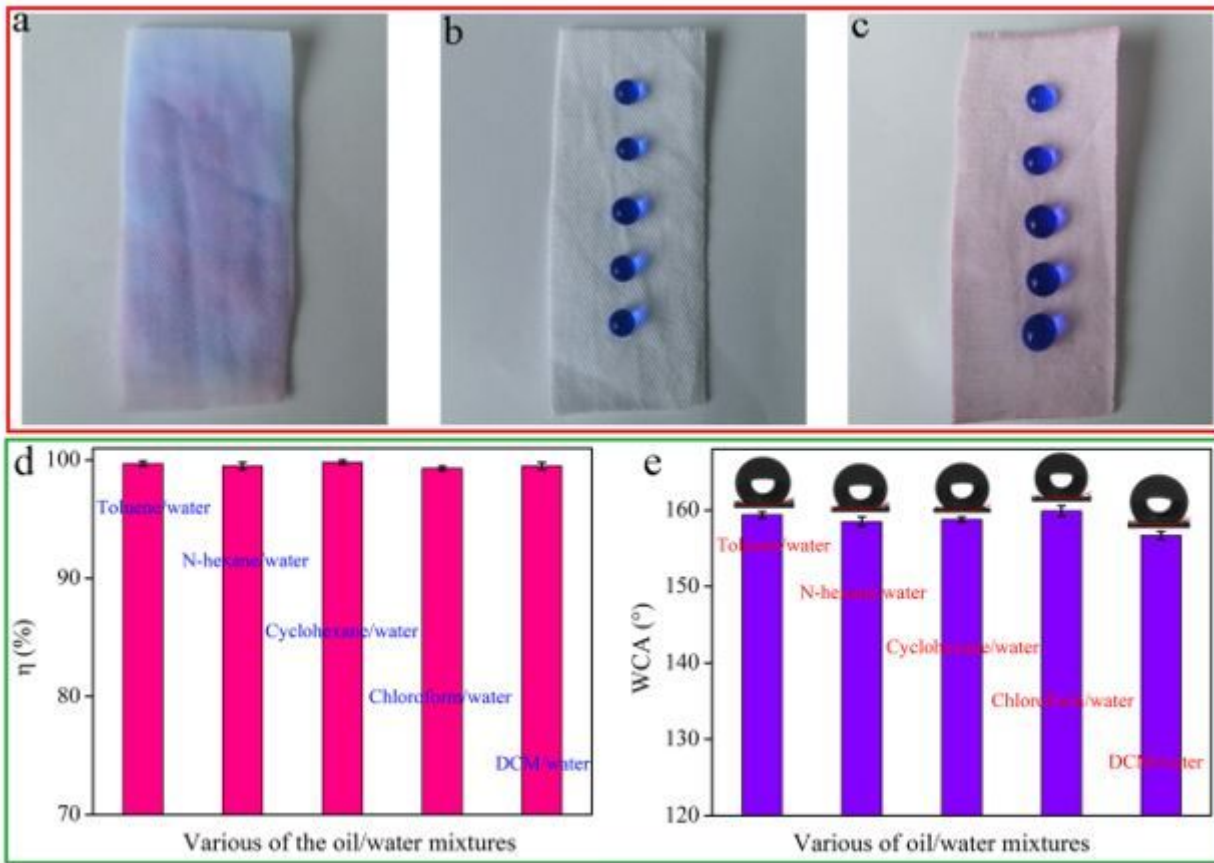


Figure 10

Water droplets (stained with ink) and chloroform (stained with oil red O) wetted on the pristine fabric (a). Water droplets placed on the SC-2 surface (b). Water droplets placed and chloroform droplets wetted on the SC-2 surface (c). Separation efficiency of SC-2 as filter material for various oil–water mixtures (d). Water contact angle of SC-2 after separation of various oil–water mixtures (e).

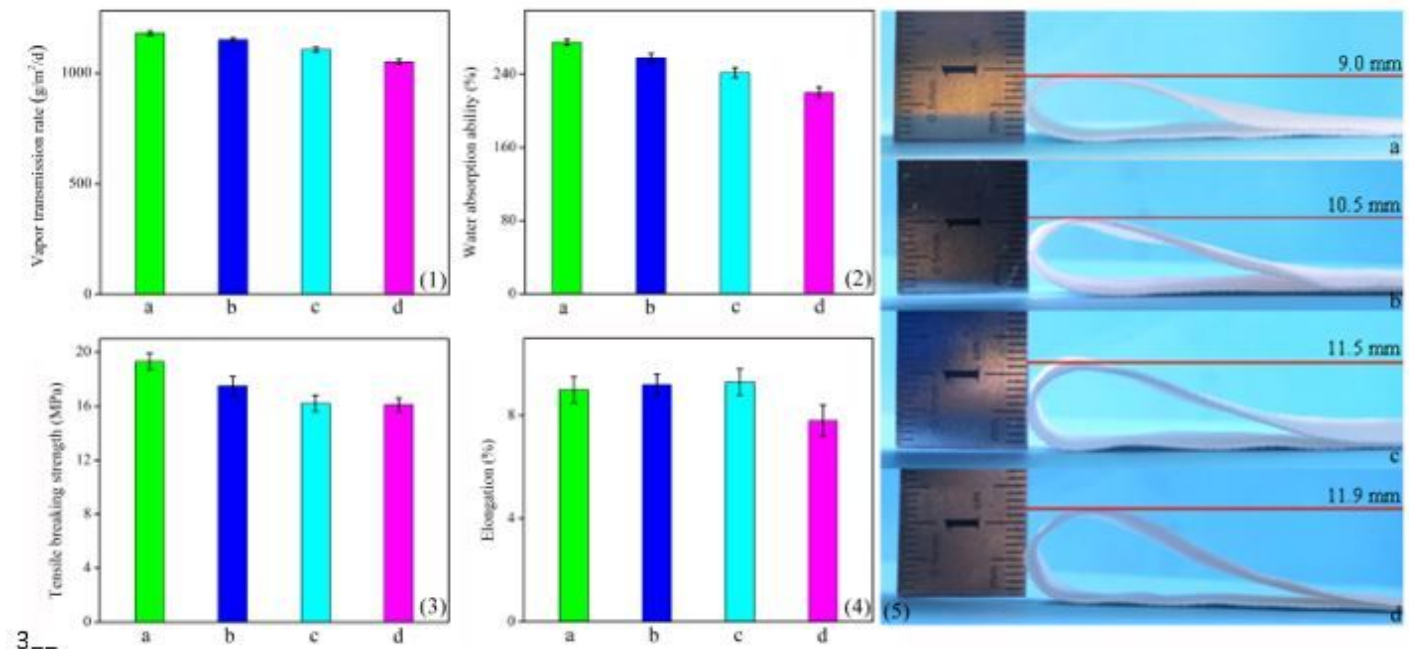


Figure 11

Water vapor permeability (1), water absorption (2), tensile strength (3), elongation (4), and flexibility (5) of the pristine fabric (a), SC-1 (b), SC-2 (c), and SC-3 (d).

Supplementary Files

This is a list of supplementary files associated with this preprint. Click to download.

- [Sl.docx](#)